Available online at www.sciencedirect.com
SCIENCE DIRECT®
Optics Communications 225 (2003) 313–318
OPTICS COMMUNICATIONS
www.elsevier.com/locate/optcom

UV-irradiation induced stress and index changes during the growth of type-I and type-IIA fiber gratings

Nguyen Hong Ky [a,*], H.G. Limberger [a], R.P. Salathé [a], F. Cochet [b], L. Dong [c]

[a] Institute of Applied Optics, Swiss Federal Institute of Technology, CH-1015 Lausanne, Switzerland
[b] Alcatel Cable Suisse S.A., CH-2016 Cortaillod, Switzerland
[c] Optoelectronics Research Centre, The University of Southampton, Southampton SO17 1BJ, UK

Received 13 May 2003; received in revised form 30 June 2003; accepted 1 July 2003

Abstract

Changes in axial stress and refractive index have been measured as a function of the total UV-irradiation fluence during the formation of Bragg gratings in B/Ge- and Sn/Ge-codoped core fibers. For the B/Ge-codoped core fiber, a fast development of the type-I grating with a significant increase in refractive index and tensile stress in the fiber core is followed by a slow growth of the type-IIA grating with a gradual decrease of refractive index and tensile core stress. A strong UV-induced reduction of the core stress and a domination of the type-IIA grating are observed for the Sn/Ge-codoped fiber. The index changes of the type-I and type-IIA gratings are believed to be governed by the compaction of the UV-irradiated core network and its dilation, respectively.

PACS: 81.40.Jj; 61.43.Fs; 42.81.Gs; 42.70.Ce

Keywords: Optical fiber; Bragg grating; Photosensitivity; Axial stress

1. Introduction

Photosensitivity of optical fibers has been extensively investigated for several years because of its important application in the fabrication of in-fiber Bragg gratings. A Bragg grating, i.e., a permanent periodic modulation of refractive index, can be formed in the core of a fiber section exposed to an interference pattern of intersecting coherent UV-light beams. During the formation of the so-called type-I grating, the index modulation amplitude, Δn, and the mean index change, $\langle \Delta n \rangle$, increase towards their saturation values with increasing total UV-irradiation fluence, F_t. The development of the type-I grating is accompanied by an increase of the axial stress in the fiber core [1,2]. This stress increase could be due to a structural transformation of the irradiated core network into a more compact configuration that is believed to be responsible for photo-induced index changes of

* Corresponding author. Present address: Corning Incorporated, SP-PR-02, Corning, NY 14831, USA. Tel.: +1-607-974-2473.
E-mail address: nguyenhk@corning.com (N.H. Ky).

0030-4018/$ - see front matter
doi:10.1016/j.optcom.2003.07.039

the type-I grating [1–4]. Evidences for structural compaction in the UV-irradiated core of Ge-doped fibers have been found by stress measurements [1,2], transmission electron microscopy (TEM) [3], interferometric microscopy [4], and Raman scattering [5]. Although the formation of the type-I grating seems to be explained by the compaction model [1–4], the formation of the type-IIA grating is not well understood. The type-IIA grating has been observed for heavily Ge-doped small-core fibers [6–8], and B/Ge- and Sn/Ge-codoped core fibers [9]. During UV irradiation of these fibers, the evolution of the type-I grating shows different stages: growth, saturation, decay and disappearance. The erasure of the type-I grating is followed by the appearance of the type-IIA grating that is characterized by negative index changes [6–9]. It was suggested [9,10] that the drawing-induced defects (DID) and the initial stress state in the fiber core may play an important role in the formation of the type-I and type-IIA gratings. The drawing tension, τ [8,9] and the strain applied to the fiber during irradiation [7] were reported to affect the axial stress in the fiber core [9] and the photosensitivity of the type-I and type-IIA gratings [7–9]. A detailed study of changes in the core stress and the photosensitivity during grating growth is very useful for understanding the origin of the type-I and type-IIA gratings. In this paper, the evolution of the index changes and the axial stress during the formation of the type-I and type-IIA gratings in the B/Ge- and Sn/Ge-codoped core fibers are reported for the first time. Our results indicate that the type-I grating is related with the compaction of the irradiated core network, whereas the type-IIA grating could be governed by the core-network dilation. The experimental techniques including the fabrication of fiber gratings and the measurements of index and stress changes are described in Section 2. The experimental results are presented and discussed in Section 3. The conclusion of this study is given in Section 4.

2. Experiment

A B/Ge-codoped core fiber and a Sn/Ge-codoped core fiber were drawn with a τ of about 75 g. Bragg gratings were written in these fibers at different F_t values using a 240-nm wavelength beam of a frequency-doubled excimer-pumped dye laser and a Lloyd interferometer. This interferometric system provides a high fringe visibility close to 100% and a good fringe stability during long irradiation time [1,11]. Pulse fluences, F_p, of 185 and 340 mJ/cm^2 were used for the irradiation of B/Ge- and Sn/Ge-codoped core fibers, respectively. The grating length, L, measured by optical low-coherence reflectometry was 1.5 ± 0.2 mm. Transmission spectra with a resolution of 0.02 nm were recorded during grating fabrication using a broad-band LED source and a monochromator. The transmission spectra permit to determine the reflectivity, R, and the Bragg wavelength, λ_B, of the gratings. $\langle \Delta n \rangle$ and Δn were deduced from the transmission data for each grating [1,9]

$$\langle \Delta n \rangle = \frac{n_{\text{eff}} \Delta \lambda_B}{\eta \lambda_B} \quad \text{and}$$

$$\Delta n = \frac{\lambda_B \operatorname{arctanh}(\sqrt{R})}{\pi \eta L}, \tag{1}$$

where $\Delta\lambda_B$ is the Bragg wavelength shift with increasing F_t, and n_{eff} and η are the effective index and the intensity fraction of light in the fiber core, respectively. The axial stress distribution across the fiber was measured using a standard technique [1,2,9,12]. The 632.8-nm wavelength beam of a He–Ne laser, linearly polarized at 45° with respect to the fiber axis, was focused to a spot of 3 μm diameter on the fiber. The stress-induced birefringence in the fiber led to a phase shift between the polarization components parallel and perpendicular to the fiber axis. The phase shift was measured as a function of the radial position of the incident beam. Since the laser beam covered several grating periods, our measurements yielded mean axial stress values, $\langle \sigma_z \rangle$, which we obtained by solving an Abel integral equation [2] that involves the phase shift.

3. Results and discussion

The radial profiles of $\langle \sigma_z \rangle$ in the B/Ge-codoped fiber (Fig. 1) consist of different regions corresponding to: (i) B/Ge-codoped core; (ii) inner

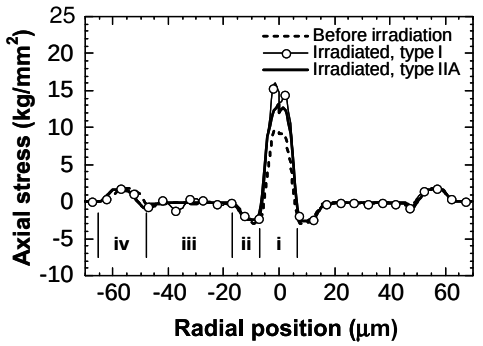

Fig. 1. Axial stress distribution in the B/Ge-codoped fiber before and after irradiation with total fluence values of 3.7 and 64.8 kJ/cm^2 corresponding to the type-I and type-IIA gratings, respectively.

cladding; (iii) substrate tube; and (iv) sleeving tube. A tensile stress (positive $\langle\sigma_z\rangle$) in the core and a compressive stress (negative $\langle\sigma_z\rangle$) in the cladding are observed because of the difference in thermal expansion coefficient of these regions [9,12]. Before irradiation, the $\langle\sigma_z\rangle$ value measured at the center of the B/Ge-codoped core is 9.4 kg/mm^2. During irradiation, $\langle\sigma_z\rangle$ changes significantly in the fiber core, whereas it remains unchanged in the cladding and the tubes. Typical $\langle\sigma_z\rangle$ profiles of the type-I and type-IIA gratings written with F_t values of 3.7 and 64.8 kJ/cm^2, respectively, are presented in Fig. 1. Fig. 2 shows Δn, $\langle\Delta n\rangle$, and $\langle\sigma_z\rangle$ of the B/Ge-codoped fiber as a function of F_t. At first, Δn and $\langle\Delta n\rangle$ increase with increasing F_t, indicating the development of the type-I grating. The growth of the type-I grating is accompanied by a strong increase of $\langle\sigma_z\rangle$. A decay of the type-I grating with a decrease in Δn is observed after the maximum Δn value of 3.7×10^{-4} is achieved at $F_t = 2.8$ kJ/cm^2. In spite of the decrease in Δn, $\langle\Delta n\rangle$ and $\langle\sigma_z\rangle$ continue to increase with increasing F_t. The maximum values $\langle\sigma_z\rangle = 15.4$ kg/mm^2 and $\langle\Delta n\rangle = 5.9 \times 10^{-4}$ are obtained at F_t values of 3.7 and 5.6 kJ/cm^2, respectively. At higher F_t, $\langle\sigma_z\rangle$ is gradually reduced, while the decrease of $\langle\Delta n\rangle$ follows that of Δn. The type-I grating disappears completely at $F_t = 12$ kJ/cm^2 where $\Delta n = 0$. After the erasure of the type-I grating, the type-IIA grating develops with increasing F_t: Δn is negative but its absolute value increases towards 4.5×10^{-4} at $F_t \approx 65$ kJ/cm^2. A correlation between $\langle\Delta n\rangle$ and $\langle\sigma_z\rangle$ is observed for both the type-I and type-IIA gratings. In fact, $\langle\Delta n\rangle$ increases with increasing $\langle\sigma_z\rangle$ during the growth of the type-I grating, while it follows well the gradual reduction of $\langle\sigma_z\rangle$ during the growth of the type-IIA grating. The UV-induced core stress, $\langle\Delta\sigma_z\rangle$, has been determined for the type-I and type-IIA gratings. The dependence of $\langle\Delta n\rangle$ on $\langle\Delta\sigma_z\rangle$ during the growth of the type-I and type-IIA gratings is shown in Fig. 3. The $\langle\Delta n\rangle$ and $\langle\Delta\sigma_z\rangle$ values of the type-I grating are positive, whereas that of the type-IIA grating are negative. However, the dependence is linear with a slope of about 0.8×10^{-4} mm^2/kg for both the type-I and type IIA-gratings. This slope value is in excellent

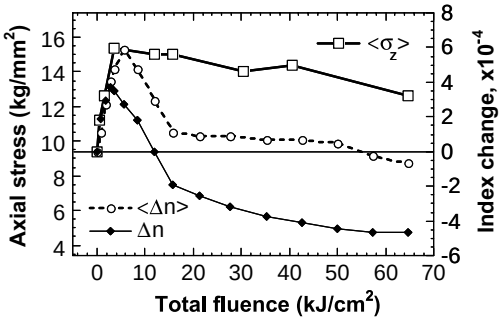

Fig. 2. Index modulation amplitude Δn, mean index change $\langle\Delta n\rangle$, and mean axial stress $\langle\sigma_z\rangle$ at the core center as a function of total irradiation fluence for gratings written in the B/Ge-codoped fiber.

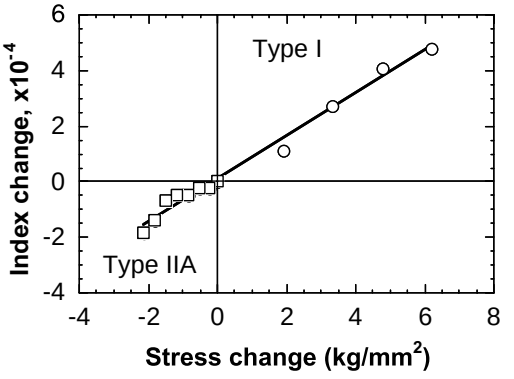

Fig. 3. Mean index change as a function of mean axial stress change at the core center for the type-I and type-IIA gratings written in the B/Ge-codoped fiber.

agreement with that reported previously for the type-I grating in Ge-doped fibers [2]. It was suggested [1] that the UV-induced index change in the fiber core during the formation of the type-I grating consists of two contributions: (i) a positive inelastic contribution, Δn_c and $\langle \Delta n_c \rangle$, due to the compaction of the irradiated core network; and (ii) a negative elastic contribution, $-\Delta n_{\sigma c}$ and $-\langle \Delta n_{\sigma c} \rangle$, induced by the axial stress change via the photo-elastic effect. Hence, Δn and $\langle \Delta n \rangle$ can be written as

$$\Delta n = \Delta n_c - \Delta n_{\sigma c}, \tag{2}$$

$$\langle \Delta n \rangle = \langle \Delta n_c \rangle - \langle \Delta n_{\sigma c} \rangle. \tag{3}$$

Since the axial stress in the core of the B/Ge-codoped fiber increases during the growth of the type-I grating, the observed increase of Δn and $\langle \Delta n \rangle$ can only be possible if the absolute values of the compaction-related inelastic contributions are larger than that of the elastic contributions. The correlation between $\langle \Delta n \rangle$ and $\langle \Delta \sigma_z \rangle$ in Fig. 3 indicates that the inelastic index changes are proportional to the axial stress. The UV-induced increase of $\langle \sigma_z \rangle$ has been reported to be due to the compaction of the core network in the irradiated regions [1,2,9]. Hence, the growth of the type-I grating in this fiber is governed by the UV-induced compaction of the core network. The compaction may be related with the transformation of the high-order ring network structure into a low-order ring structure through the annihilation of oxygen-deficient centers (ODC) [5]. The initial ODC concentration in the core of this fiber has been suggested to be relatively high because of a low tensile stress and a reduced viscosity caused by B codoping in the core [9,12]. In addition, B codoping is favorable for the annihilation of ODCs during UV irradiation [9,12]. Since the irradiation profile along the fiber is generally assumed to be sinusoidal-like with sequential irradiated and dark sections, the largest value of Δn could be achieved first at the central region of each irradiated section where the maximum degree of compaction is attained. As the irradiation is continued, the region with maximum degree of compaction is widened until it covers the whole irradiated section. As a consequence, the increase of $\langle \Delta n \rangle$ and $\langle \sigma_z \rangle$ remains after the maximum value of Δn has been achieved (Fig. 2). The decrease in Δn appears, indicating that the volume dilation of the core network may begin in the region with highest degree of compaction. The volume dilation seems to begin when a depletion of ODCs and a high tensile stress develop in the core as a result of the UV-induced compaction. The volume dilation introduces negative inelastic index changes, $-\Delta n_d$ and $-\langle \Delta n_d \rangle$, and positive elastic index changes caused by a reduction of the axial stress. Eqs. (2) and (3) may become

$$\Delta n = \Delta n_c - \Delta n_d - \Delta n_{\sigma c} + \Delta n_{\sigma d}, \tag{4}$$

$$\langle \Delta n \rangle = \langle \Delta n_c \rangle - \langle \Delta n_d \rangle - \langle \Delta n_{\sigma c} \rangle + \langle \Delta n_{\sigma d} \rangle. \tag{5}$$

The dilation and the compaction could occur simultaneously: the central region of the irradiated section is dilated whereas the regions near its edges are compacted. After the tensile stress in the fiber core attains its limit with the observation of the maximum $\langle \sigma_z \rangle$ value and the maximum degree of compaction is achieved at the edges of the irradiated section, only the volume dilation remains. As the volume dilation develops towards the edges of the irradiated section, $\langle \Delta n \rangle$ and $\langle \sigma_z \rangle$ decrease. The type-I grating is completely erased when the compaction-related index changes are compensated by the dilation-related index changes. The appearance of the type-IIA grating seems to be related with a domination of the volume dilation

$$\Delta n = -\Delta n_d + \Delta n_{\sigma d}, \tag{6}$$

$$\langle \Delta n \rangle = -\langle \Delta n_d \rangle + \langle \Delta n_{\sigma d} \rangle. \tag{7}$$

Our results obtained for the Sn/Ge-codoped core fiber confirm that the ODC depletion and the high tensile stress play an important role in the volume-dilation induced type-IIA grating. The use of Sn as a codopant with Ge leads to an increase in the melting temperature and the viscosity of the core. As a consequence, a high tensile stress is expected in the core where DIDs rather than ODCs are dominant defects [9,12]. The $\langle \sigma_z \rangle$ profiles of Sn/Ge-codoped fiber in Fig. 4 show that the $\langle \sigma_z \rangle$ value measured at the core center (i) before irradiation is as large as 15.3 kg/mm^2 comparable to the maximum $\langle \sigma_z \rangle$ value that can be achieved in

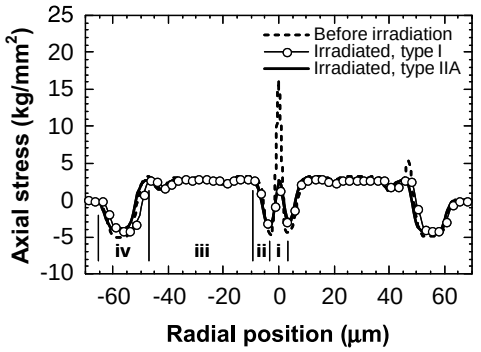

Fig. 4. Axial stress distribution in the Sn/Ge-codoped fiber before and after irradiation with total fluence values of 0.3 and 22 kJ/cm^2 corresponding to the type-I and type-IIA gratings, respectively.

the B/Ge-codoped fiber after irradiation. A high axial tensile stress and a low ODC concentration should inhibit the compaction [3,9]. On the contrary, this condition may be favorable for the dilation process in the Sn/Ge-codoped core. The evolution of Δn, $\langle \Delta n \rangle$, and $\langle \sigma_z \rangle$ as a function of F_t is shown in Fig. 5 for the Sn/Ge-codoped fiber. The compaction-related type-I grating quickly attains its maximum Δn value of 1.46×10^{-4} at $F_t =$ 1 kJ/cm^2 and the dilation begins with a decrease in Δn that is accompanied by a strong $\langle \sigma_z \rangle$ reduction of 13.8 kg/mm^2. With increasing F_t, the $\langle \sigma_z \rangle$ value in the core remains between 1.5 and 2.6 kg/mm^2 that is close to the $\langle \sigma_z \rangle$ value of 2.5 kg/mm^2 in the substrate tube (Region iii, Fig. 4). There is no

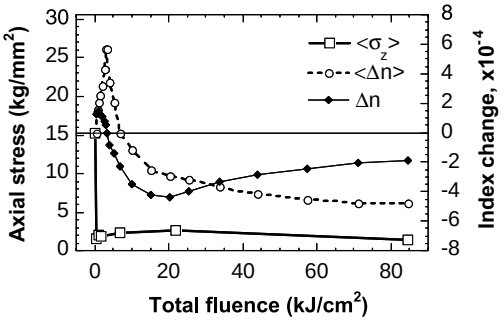

Fig. 5. Index modulation amplitude Δn, mean index change $\langle \Delta n \rangle$, and mean axial stress $\langle \sigma_z \rangle$ at the core center as a function of total irradiation fluence for gratings written in the Sn/Ge-codoped fiber.

correlation between $\langle \Delta n \rangle$ and $\langle \sigma_z \rangle$, indicating that the stress-induced photo-elastic contribution to the index change could be negligible. At $F_t = 3$ kJ/cm^2, the type-I grating is erased completely and the type-IIA grating appears with a $\langle \Delta n \rangle$ decrease. The maximum Δn value of -4.4×10^{-4} is achieved at $F_t = 20.3$ kJ/cm^2 for the type-IIA grating. Hence, the type-IIA grating could be governed by the volume dilation in the Sn/Ge-codoped core. Our results agree well with that of [3] where TEM observations of the type-I gratings in the Sn/Ge-codoped core indicate that UV-induced compaction occurs but it is significantly weaker than in the Ge-doped core. Opened micro-cracks are observed in the UV-irradiated Sn/Ge-codoped core. Cordier et al. [3] suggested that the opening of cracks perpendicular to the fiber axis relaxes the Sn/Ge-codoped core which is under a high axial tensile stress. An increase of compressive stress during the growth of the type-IIA gratings in planar germanosilicate waveguides has been reported by Canning and Aslund [13]. Their observation has been explained by structural change through inelastic dilation of the glass in the region of peak irradiation [13].

4. Conclusion

The evolution of Δn, $\langle \Delta n \rangle$, and $\langle \sigma_z \rangle$ during the formation of the type-I and type-IIA gratings in B/Ge- and Sn/Ge-codoped core fibers has been investigated. The UV-irradiation induced compaction of the core network is confirmed to be the origin of the type-I grating. The structural compaction leads to an increase of Δn, $\langle \Delta n \rangle$, and $\langle \sigma_z \rangle$ during the growth of the type-I grating. Moreover, our results show that the dilation of the core network could be responsible for the type-IIA grating characterized by a reduction of Δn, $\langle \Delta n \rangle$, and $\langle \sigma_z \rangle$ during its growth. The depletion of ODCs and the high tensile stress in the fiber core are believed to be favorable for the dilation-related type-IIA grating. A correlation between $\langle \Delta n \rangle$ and $\langle \Delta \sigma_z \rangle$ is observed for both the type-I and type-IIA gratings in the B/Ge-codoped core fiber. The absence of this correlation in the Sn/Ge-codoped fiber may be due to the relaxation of the high tensile stress in its core.

Acknowledgements

We thank C. Oliveira for her technical supports. This work was supported by the European AC046 ACTS PHOTOS Project.

References

[1] H.G. Limberger, P.Y. Fonjallaz, R.P. Salathé, F. Cochet, Appl. Phys. Lett. 68 (1996) 3069.
[2] P.Y. Fonjallaz, H.G. Limberger, R.P. Salathé, F. Cochet, B. Leuenberger, Opt. Lett. 20 (1995) 1346.
[3] P. Cordier, S. Dupont, M. Douay, G. Martinelli, P. Bernage, P. Niay, J.F. Bayon, L. Dong, Appl. Phys. Lett. 70 (1997) 1204.
[4] B. Poumellec, P. Niay, M. Douay, J.F. Bayon, J. Phys. D 29 (1996) 1842.
[5] E.M. Dianov, Y.N. Pyrkov, V.G. Plotnichenko, V.V. Koltashev, N.H. Ky, H.G. Limberger, R.P. Salathé, Opt. Lett. 22 (1997) 1754.
[6] W.X. Xie, P. Niay, P. Bernage, M. Douay, J.F. Bayon, T. Georges, M. Monerie, B. Poumellec, Opt. Commun. 104 (1993) 185.
[7] T. Taunay, P. Niay, P. Bernage, M. Douay, W.X. Xie, D. Pureur, P. Cordier, J.F. Bayon, H. Poignant, E. Delevaque, B. Poumellec, J. Phys. D 30 (1997) 40.
[8] I. Riant, B. Poumellec, Fiber Integrated Opt. 18 (1999) 15.
[9] N.H. Ky, H.G. Limberger, R.P. Salathé, F. Cochet, L. Dong, Opt. Lett. 23 (1998) 1402.
[10] W.X. Xie, P. Niay, P. Bernage, M. Douay, T. Taunay, J.F. Bayon, E. Delevaque, M. Monerie, Opt. Commun. 124 (1996) 295.
[11] H.G. Limberger, P.Y. Fonjallaz, R.P. Salathé, Electron. Lett. 29 (1993) 47.
[12] N.H. Ky, H.G. Limberger, R.P. Salathé, F. Cochet, L. Dong, Appl. Phys. Lett. 74 (1999) 516.
[13] J. Canning, M. Aslund, Opt. Lett. 24 (1999) 463.